Electronic collective modes and instabilities on semiconductor surfaces. I

A. Muramatsu

Institute for Theoretical Physics, University of California, Santa Barbara, California 93106

W. Hanke

Max-Planck-Institut für Festkörperforschung, D-7000 Stuttgart 80, West Germany
and Institute for Theoretical Physics, University of California, Santa Barbara, California 93106

A Green's-function theory of electronic collective modes is presented which leads to a practical scheme for a microscopic determination of surface elementary excitations in conducting as well as nonconducting solids. Particular emphasis is placed on semiconductor surfaces where the jellium approximation is not valid, due to the importance of density fluctuations on a microscopic scale (reflected in the local-field effects). Starting from the Bethe-Salpeter equation for the two-particle Green's function of the surface system, an equation of motion for the electron-hole pair is obtained. Its solutions determine the energy spectra, lifetimes, and amplitudes of the surface elementary excitations, i.e., surface plasmons, excitons, polaritons, and magnons. Exchange and correlation effects are taken into account through the random-phase and time-dependent Hartree-Fock (screened electron-hole attraction) approximations. The formalism is applied to the study of electronic (charge- and spin-density) instabilities at covalent semiconductor surfaces. Quantitative calculations for an eight-layer Si(111) slab display an instability of the ideal paramagnetic surface with respect to spin-density waves with wavelength nearly corresponding to (2×1) and (7×7) superstructures.

I. INTRODUCTION

Elementary excitations constitute a fundamental tool to study the dynamics of interacting many-particle systems. The description of such excitations in terms of a unifying physical concept has been provided by the Green's-function formalism and especially by the linear-response theory. These facts were established first by the pioneering work of Pines and Nozières[1,2] and many others for the homogeneous electron gas. This model proved to be successful for systems where the valence-electron density is essentially constant, as in simple metals. However, in the case of bulk solids, with more or less localized electronic states, new effects due to the inhomogeneity of the electronic charge distribution appear. These effects were shown[3-6] to be a manifestation of microscopic density fluctuations induced by the periodicity of the charge distribution while responding to a macroscopic external field. An essential point of our theoretical study of these effects in bulk[3-6] has been to demonstrate the intimate interrelation between the electronic localization or inhomogeneity of the charge density and the importance of many-body effects.

In the case of a surface, the charge inhomogeneity is inherent in the system and it is then expected that the many-body effects become even more pronounced than in bulk. In fact, Jonson and Srinivasan[7] found for a jellium-slab model with infinite barriers that the correlation energy is more dominant in the surface [$\sim 1/(r_s)^{1/2}$] than in the bulk ($\sim \ln r_s$) in the high-density limit.

One aim of the present work is to study the many-body interactions on surfaces, taking into account both the charge-density fluctuations due to the surface itself and to the presence of a lattice. In order to attain this objective we develop a microscopic description of elementary excitations on surfaces, starting from one-electron energies and wave functions and incorporating the correlation terms according to the field-theoretical prescription (Feynman-Dyson perturbation theory[8]), as in bulk.[3-5] Previous descriptions of surface response functions and elementary excitations[9] have several limitations, due in part to the imposition of macroscopic boundary conditions or artificial surface profiles. These approximations can severely affect some physical properties, such as the dispersion of surface elementary excitations, as Feibelman[10] has shown in the case of surface plasmons. Another restriction in these studies is given by the random-phase approximation (RPA), which, on grounds of our experience in bulk,[3-6] is not expected to be a good approximation for semiconductor surfaces.

In Sec. II we outline first a local-orbital treatment of the two-particle Green's function for the surface, where the irreducible electron-hole interaction contains the RPA local-field effects and the screened electron-hole attraction. Both contributions are of crucial importance in bulk to explain quantitatively the optical spectrum,[3,4] static,[6] and dynamical[5] screening of covalent semiconductors, the latter being decisive for an accurate evaluation of the one-particle spectrum of those systems.[5] With the definition of an amplitude of collective excitations, in the same way as done by Sham and Rice[11] for bulk Wannier excitons, we obtain a solvable equation of motion for the electron-hole pair starting from the Bethe-Salpeter equation. The solutions of this equation of motion determine the energy spectrum, lifetime, and amplitudes of the collective excitations.

Armed with the knowledge of the elementary excitation spectrum, we focus on the problem of electronic instabilities in surface systems using the same formalism. This interest arises from the fact that, in a simplified one-electron picture (and neglecting electron-phonon interaction), the creation of an ideal surface can lead to a system with properties at the surface radially different from the bulk. One example, which will be discussed in detail, is the surface of covalent semiconductors, specifically the Si(111) surface. In this system the ideal surface geometry gives rise to a half-filled metallic band on top of the semiconducting substrate if one uses an independent-particle model. In contrast to this, a reconstructed surface with nonmetallic properties is observed experimentally.

Our formalism allows for a stringent test of the surface stability when exchange and correlation are carefully taken into account. The idea is that, if the excitation energy of a collective mode tends to zero, the ground state itself has to incorporate this collective state,[12] signaling an electronic instability.

For the application, we choose the Si(111) surface which has been extensively studied in the past[13] and nevertheless is still a source of continued and partly controversial arguments both experimentally[14,15] and theoretically.[16-18] Recent angle-resolved photoemission experiments for the (2×1) cleaved surface[14] proposed the existence of two nearly dispersionless surface states, and suggested that correlation effects might be important for the surface. On the other hand, new data obtained by the same technique have been assigned to a highly dispersive dangling-bond (DB) band. On the theoretical side, pseudopotential local-spin-density calculations[16] found that a nonbuckled antiferromagnetic surface is stable against buckling-type distortions. Two occupied surface states are obtained when buckling is introduced, which has been suggested to be stabilized by steps on the freshly cleaved surface. Independently, a π-bonded—chain model was proposed by Pandey[17] which lowers the energy of the system even further.[18] Furthermore, a potential barrier (~ 0.05 eV per surface atom) has to be crossed in going from the lowest-state configuration in Ref. 15 to the equilibrium configuration of the π-bonded—chain model.[19]

For this specific system our intention is to study the mechanism that initially drives the electronic system out of its ideal configuration. Emphasis is put on a Green's-function treatment of the many-body interactions, where we can consider the nonlocality in exchange and correlation in the presence of the surface, as opposed to the local-density-type studies described before. Confirming our above expectations, we find the many-particle interactions to become more pronounced at the Si(111) surface than in the bulk. Our numerical results demonstrate, for the ideal surface, that these interactions drive the system into a spin-density-wave (SDW) instability, which cannot be obtained only on the basis of the band-structure (Fermi-surface—nesting) effect. This instability develops at wavelengths corresponding to (2×1) and (7×7) superstructures, where the (2×1) antiferromagnetic SDW is in accordance with the findings of Ref. 16. Since we can deal only with small distortions of the ideal configuration

and not appreciable changes as proposed in Ref. 17, we are not able to obtain the new ground-state configuration. However, starting, for example, from the proposed equilibrium configuration of the π-bonded—chain model, our formalism can be used to obtain its elementary excitation spectrum and check it against experiment.

In Sec. III we give the details of the calculation. The numerical results are discussed in Sec. IV, and summary and conclusions are finally given in Sec. V.

II. EQUATION OF MOTION AND INSTABILITIES

In this section we obtain (a) a practical solution of the equation of motion (EOM) for the collective excitations of a surface system, and (b) the conditions under which the surface electronic system becomes unstable with respect to a metal-insulator transition. The first result is achieved by first defining an amplitude of the collective excitations[2,11,12] which fulfills an integral equation derived from the homogeneous Bethe-Salpeter equation for the two-particle Green's function. The second step consists of introducing an expansion of the surface Block states in localized orbitals. The condition for an electronic instability is attained whenever a collective excitation can arise without having delivered any energy to the system. That is, we have to look for elementary excitations with excitation energy $\omega = 0$.[12]

A. Equation of motion of surface elementary excitations

The microscopic description of elementary excitations in many-particle systems is given by the two-particle Green's function for the electron-hole pair,[2] which for finite temperatures is defined as[8,20]

$$G(1,2;3,4) = \langle T_\tau \widetilde{\psi}(1) \widetilde{\psi}(2) \widetilde{\psi}^\dagger(3) \widetilde{\psi}^\dagger(4) \rangle , \qquad (1)$$

where $1 \equiv (\vec{r}, \tau_1)$

$$\widetilde{\psi}(1) = e^{(H-\mu N)\tau_1} \psi(\vec{r}_1) e^{-(H-\mu N)\tau_1} . \qquad (2)$$

N is the particle number operator and T_τ is the time-ordering operator. H is the many-body Hamiltonian and we consider the limit $T \to 0$. This limiting procedure allows us to define the chemical potential μ unambiguously for $T = 0$.[8,11]

The system is taken as periodic in directions parallel to the surface. This fact allows us to characterize the eigenstates of the many-body Hamiltonian in the following way:

$$H \mid N, n, \vec{k} \rangle = E_{N,n,\vec{k}} \mid N, n, \vec{k} \rangle , \qquad (3)$$

where $\vec{k}$ is a two-dimensional (2D) wave vector parallel to the surface and belongs to the first 2D Brillouin zone. n stands for all other quantum numbers which specify the corresponding state. $\mid N, 0 \rangle$ is the exact ground state of the N-particle system. $G(1,2;3,4)$ can be divided into a free and a bound part,[2]

$$G(1,2;3,4) = G(1,3)G(2,4) - G(1,4)G(2,3)$$

$$+ \delta G(1,2;3,4) . \qquad (4)$$

The free part, which is given by the first two terms, corresponds to the propagation of two excitations totally independent of one another, resulting in a product of two one-particle Green's functions, where the indistinguishability of the particles should be taken into account. On the other hand, the bound part $\delta G(1,2;3,4)$ describes the interaction of these two excitations and contains new information that is not explicitly given in the one-particle Green's function $G(1,2)$.

In order to formulate an equation of motion for surface elementary excitations and to introduce notations needed in the following discourse, we shall first follow the work by Sham and Rice closely.[11] We start with the Bethe-Salpeter equation (Fig. 1) satisfied by the bound part $\delta G(1,2;3,4)$,[2,11]

$$\delta G(1,2;3,4)=G(2,2')G(3',3)I(1',2';3',4')G(1,1')G(4',4)$$
$$+G(2,2')G(3',3)I(1',2';3',4')\delta G(1,4';1',4),$$

$$(5)$$

where $I(1',2',3',4')$ is the irreducible electron-hole interaction and integrations over repeated arguments are understood. The solutions of this integral equation[4] determine, in principle, the dynamics of the electron-hole pair
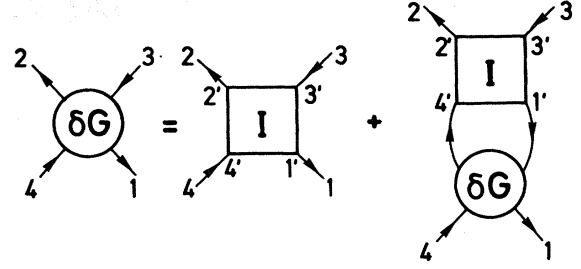

FIG. 1. Bethe-Salpeter integral equation for the bound part δG of the two-particle Green's function.

completely. However, being primarily interested in the collective modes of the system, we will concentrate on the poles of $\delta G(1,2;3,4)$. We assume that there exists a collective excitation described by the state $|N,\lambda,\vec{q}\rangle$, with excitation energy $\omega_{\lambda,\vec{q}}=E_{N,\lambda,\vec{q}}-E_{N0}$. This is an eigenstate of the system, implying that $|N,\lambda,\vec{q}\rangle$ has no damping and ω is real. In the case of an unstable bound state, the pole at $\omega_{\lambda,\vec{q}}$ will be complex, its imaginary part characterizing the damping produced by the decay of such a state into the continuum of other excitations

The $\vec{q}$ component of the bound part δG is given by[11]

$$\delta G_{\vec{q}}(1,2;3,4)=2\pi i\delta(\omega_1+\omega_2-\omega_3-\omega_4)\left[\frac{G_{0,\lambda-\vec{q}}(1,4)G_{\lambda,-\vec{q},0}(2,3)}{\omega_2-\omega_3+E_{N,\lambda,-\vec{q}}-E_{N0}}-\frac{G_{0,\lambda,\vec{q}}(2,3)G_{\lambda,\vec{q},0}(4,1)}{\omega_2-\omega_3+E_{N0}-E_{N,\lambda,\vec{q}}}+\cdots\right],$$

$$(6)$$

with

$$G_{0,\lambda,\vec{q}}(2,3)=\sum_\alpha\left[\frac{\langle N,0|\psi(\vec{r}_2)|N+1,\alpha\rangle\langle N+1,\alpha|\psi^\dagger(\vec{r}_3)|N,\lambda,\vec{q}\rangle}{\omega_2+E_{N0}-E_{NH,\alpha}}\right.$$

$$\left.-\frac{\langle N,0|\psi^\dagger(\vec{r}_3)|N-1,\alpha\rangle\langle N-1,\alpha|\psi(\vec{r}_2)|N,\lambda,\vec{q}\rangle}{-\omega_3+E_{N0}-E_{N-1,\alpha}}\right].$$

$$(7)$$

The terms in large parentheses in Eq. (6) are obtained using the spectral representation of the 24 terms that are obtained through all possible permutations in (1).[11] Explicitly written are those terms that will contribute to the singular terms in $\delta G_{\vec{q}}$ for $\omega_{\lambda,\vec{q}}=E_{N,\lambda,\vec{q}}-E_{N0}$. Only these contributions need to be considered in the integral Eq. (5). The first term on the right-hand side of Eq. (5) is regular and can be neglected. Inserting expression (6) in Eq. (5), the homogeneous Bethe-Salpeter equations are obtained,[11]

$$G_{0,\lambda,\vec{q}}(2,3)=G(2,2')G(3',3)I(1',2';3',4')G_{0,\lambda,\vec{q}}(4',1'),$$

$$(8a)$$

with $\omega_2-\omega_3=E_{N,\lambda,\vec{q}}-E_{N0}$, and

$$G_{\lambda,\vec{q},0}(4,1)=G_{\lambda,\vec{q},0}(3',2')I(1',2';3',4')G(1,1')G(4',4),$$

$$(8b)$$

with $\omega_4-\omega_1=E_{N,\lambda,\vec{q}}-E_{N0}$. These equations determine the excitation energy and amplitude of the elementary excitation. This can be seen from the definition of the amplitude of the collective mode,[11]

$$f_{\lambda,\vec{q}}(\vec{r}_2,\vec{r}_3)=\langle N,0|\psi^\dagger(\vec{r}_3)\psi(\vec{r}_2)|N,\lambda,\vec{q}\rangle,$$

$$(9)$$

and the following identity:

$$\langle N,0|\psi^\dagger(\vec{r}_3)\psi(\vec{r}_2)|N,\lambda,\vec{q}\rangle=\lim_{\eta\to0^+}\frac{1}{2\pi i}\int_c d\omega_2 e^{\omega_2\eta}G_{0,\lambda,\vec{q}}(\vec{r}_2,\omega_2;\vec{r}_3,\omega_2-\omega),$$

$$(10)$$

with the contour of integration c given by Ref. 11. The identity (10) can be used to obtain an integral equation for $f_{\lambda,\vec{q}}$ from Eq. (8a),[11]

$$f_{\lambda,\vec{q}}(\vec{r}_2,\vec{r}_3)=\int d^3r'_1\cdots d^3r'_4 \left[\sum_{n,n',\vec{k}} \frac{\varphi_{n,\vec{k}+\vec{q}}(\vec{r}_2)\varphi^*_{n,\vec{k}+\vec{q}}(\vec{r}'_2)\varphi^*_{n',\vec{k}}(\vec{r}_3)\varphi_{n',\vec{k}}(\vec{r}'_3)}{\omega-E_N(\vec{k}+\vec{q})+E_{n'}(\vec{k})} \right.$$

$$\left. \times [f_n(\vec{k}+\vec{q})-f_{n'}(\vec{k})] \right] I(\vec{r}'_1,\vec{r}'_2;\vec{r}'_3,\vec{r}'_4)f_{\lambda,\vec{q}}(\vec{r}'_4,\vec{r}'_1) , \tag{11}$$

where we restrict ourselves to a screened Hartree-Fock approximation for the irreducible electron-hole interaction[4] (Fig. 2),

$$I(1',2';3',4')=-\delta(1',3')\delta(2',4')V^s(2',3')+\delta(1',4')\delta(2',3')V(2',4') . \tag{12}$$

$I(1',2';3',4')$ is time independent, since only a static screening is taken into account in V^s.[4] Thus, we arrived at an equation of motion for the amplitude (wave function) of the collective excitations. We reproduced the derivation[11] of Sham and Rice for the sake of clarity, Eq. (11) being the starting point to obtain a solvable equation of motion with the help of a local representation for the surface Block states.

B. Equation of motion in the local-orbital representation

We introduce here a local-orbital representation for the surface Block wave functions. The use of a tight-binding basis has already proved to be extremely useful for bulk covalent semiconductors,[3-6] where "jellium"-type approximations are not valid. In tight binding, the Bethe-Salpeter equation is cast in a matrix form which can be solved by inversion. The form of the expansion in our case is the following:

$$\varphi_{n,\vec{k}}(\vec{r})=\frac{1}{\sqrt{NM}} \sum_{m,v} c^m_{nv}(\vec{k}) \sum_l e^{i\vec{k}\cdot\vec{R}_l}a^m_v(\vec{r}-\vec{R}_m-\vec{R}_l) , \tag{13}$$

where m denotes the mth layer in a thin slab with M layers, $\vec{R}_l$ is a two-dimensional (2D) translation vector, $\vec{R}_m$ is a 3D basis vector for the 2D unit cell, v is an orbital index, and N is the number of 2D unit cells. Similarly, the wave functions of the collective modes are also expanded in a set of localized orbitals,

$$f_{\lambda,\vec{q}}(\vec{r}_2,\vec{r}_3)=\frac{1}{NM} \sum_{v,v'} a_v(\vec{r}_2-\vec{R}_m-\vec{R}_l)a^*_{v'}(\vec{r}_3-\vec{R}_{m'}-\vec{R}_{l'})e^{i\vec{q}\cdot\vec{R}_l}F_s , \tag{14}$$

where F_s defines the amplitude "per site" of the collective excitation. The index s is short for $s\equiv(v,v',m,m',\vec{R}_l-\vec{R}_{l'})$.

Substituting expressions (13) and (14) in the integral equation (11), we obtain a matrix equation,

$$\sum_{l'} e^{i\vec{q}\cdot\vec{R}_{l'}} \sum_{s,s',s''} \alpha^m_v(\vec{r}_2-\vec{R}_m-\vec{R}_s-\vec{R}_{l'})[a^{m'}_{v'}(\vec{r}_3-\vec{R}_{m'}-\vec{R}_{l'})]^*(F_s+N_{ss'}V^{xc}_{s's''}F_{s''})=0 . \tag{15}$$

The matrix $N_{ss'}$ in Eq. (15) is given by

$$N_{s_1 s_2}(\vec{q},\omega)=\frac{1}{NM} \sum_{n,n',\vec{k}} c^{m_1}_{n_1 v_1}(\vec{k}+\vec{q})[c^{m'_1}_{n'_1 v'_1}(\vec{k})]^* e^{i(\vec{k}+\vec{q})\cdot\vec{R}_{s_1}}$$

$$\times \frac{f_n(\vec{k}+\vec{q})-f_{n'}(\vec{k})}{E_n(\vec{k}+\vec{q})-E_{n'}(\vec{k})-\omega-i\eta} e^{-i(\vec{k}+\vec{q})\cdot\vec{R}_{s_2}}[c^{m_2}_{nv_2}(\vec{k}+\vec{q})]^* c^{m'_2}_{n'v'_e}(\vec{k}) . \tag{16}$$

This quantity contains the information about the one-particle excitations (band structure) of the system. The two-particle many-body effects are contained in

$$V^{xc}_{ss'}=-V^c_{ss'}+\tfrac{1}{2}V^s_{ss'} , \tag{17}$$

with

$$V^c_{ss'}(\vec{q})=\sum_p e^{-i\vec{q}\cdot\vec{R}_p} \int\int d^3r\,d^3r'a^*_\mu(\vec{r}-\vec{R}_l-\vec{R}_p)a_v(\vec{r}-R_p)v(\vec{r}-\vec{r}')a^*_{v'}(\vec{r}')a_{\mu'}(\vec{r}'-\vec{R}_{l'}) , \tag{18}$$

where $\vec{R}_p$ is a 2D translation vector. V^c is the exchange interaction to the electron-hole attraction,[5] and is represented in Fig. 2(b). It gives rise to the local-field effects, a fact that can be seen from Eq. (18) where V^c is expressed as a summation of the interactions of a "dipole" (electron-hole pair) at the lattice site $\vec{R}=\vec{0}$ with "dipoles" at lattice sites $\vec{R}=\vec{R}_p$

which are induced through the motion of a collective excitation along the system. Owing to the long-range nature of this repulsive interaction, it is convenient to calculate this quantity in 2D reciprocal space. The corresponding form is

$$V^c_{ss'} = \sum_{\vec{G}} \int \int dz\, dz' A_s^\dagger(\vec{q}+\vec{G},z)v(\vec{q}+\vec{G},|z-z'|)A_{s'}(\vec{q}+\vec{G},z') , \tag{19}$$

where $A_s(\vec{q}+\vec{G},z)$ is a generalized charge-density wave,

$$A_s(\vec{q}+\vec{G},z) = \int d^2r\, [a_v^m(\vec{r},z-R_m^z)]^* e^{-i(\vec{q}+\vec{G})\cdot\vec{r}} a_{v'}^{m'}(\vec{r}-\vec{R}_s,z-R_{m'}^z) , \tag{20}$$

G is a 2D reciprocal-lattice vector, and $\vec{r}$ is a 2D vector parallel to the surface, the coordinates z and z' being perpendicular to the surface. The interaction potential between the charge-density waves is the 2D Fourier-transformed Coulomb potential,

$$v(\vec{q}+\vec{G},|z-z'|) = 2\pi e^2 \frac{e^{-|\vec{q}+\vec{G}||z-z'|}}{|\vec{q}+\vec{G}|} . \tag{21}$$

Finally, the matrix $V^s_{ss'}$ is given by

$$V^s_{s'}(\vec{q}) = \sum_p e^{-i\vec{q}\cdot\vec{R}_p} \int \int \int d^3r\, d^3r'\, d^3r'' a_\mu^*(\vec{r}-\vec{R}_l-\vec{R}_p)a_v(\vec{r}'-\vec{R}_p)v(\vec{r}-\vec{r}'')\epsilon^{-1}(\vec{r}'',\vec{r}')a_{v'}^*(\vec{r}'')a_{\mu'}(\vec{r}'-\vec{R}_{l'}) . \tag{22}$$

It corresponds to the statically screened electron-hole attraction, represented by Fig. 2(a).

The matrices $\underline{N}$, $\underline{V}^c$, and $\underline{V}^s$ described above are the 2D versions of the equivalent quantities obtained by Hanke and Sham[3,4] in the study of optical properties in the bulk of covalent semiconductors. The fact that Eq. (15) is valid for any complete local basis allows a very simple form of the equation of motion for the collective excitations,

$$[1+\underline{N}(\vec{q},\omega)\underline{V}^{xc}(\vec{q})]\vec{F}(\vec{q}) = \vec{0} , \tag{23}$$

which is subjected to the condition

$$\det[1+\underline{N}(\vec{q},\omega)\underline{V}^{xc}(\vec{q})] = 0 . \tag{24}$$

These solutions determine in a completely general way the energy spectrum and amplitude of the eigenmodes of charge-density fluctuations on the surface, i.e., surface plasmons as longitudinal elementary excitations, or also surface excitons with longitudinal as well as transverse character. The realization of the method presented is limited in practice by the size of the matrices $\underline{N}$ and $\underline{V}^{xc}$. As a consequence of this constraint, calculations can be performed only for relatively thin slabs. Moreover, the wave functions of the system should be sufficiently localized to allow the use of a few overlaps in the density form factors (20). Finally, the extension of the electron-hole pairs entering in the interaction V^s of (22) should be limited to a lattice distance (Frenkel and intermediate-radius excitons). In Secs. III and IV we will discuss these aspects in connection with numerical studies of an ideal Si(111) eight-layer slab.

Electronic instabilities

We now consider the conditions under which an instability of the surface electronic system develops. The situation arises when the excitation energy of an isolated elementary excitation (plasmon, exciton, etc.) or of a well-defined peak inside a continuum decreases drastically for a certain wave vector $\vec{q}_0$, giving as a result increasingly important charge- (or spin-) density fluctuations with wavelength $2\pi/q_0$. When the excitation energy $\omega(\vec{q}_0)$ becomes zero, the system undergoes an electronic instability.

Recalling the condition (24) for $\omega = 0$, we obtain

$$\det[\underline{N}^{-1}(\vec{q},\omega=0)+\underline{V}^{xc}(\vec{q})] = 0 \tag{25}$$

as the condition corresponding to an instability of the system against formation of a charge-density wave (CDW) of wavelength $2\pi/q$. As can be seen in Fig. 2, the term V^{xc} contains the contributions for an electron-hole pair in the singlet configuration. In the case of a triplet configuration, that is, for a spin-density wave (SDW), we obtain a similar condition,

$$\det[\underline{N}^{-1}(\vec{q},\omega=0)+\tfrac{1}{2}\underline{V}^s(\vec{q})] = 0 . \tag{26}$$

The interaction term V^c [Fig. 2(b)] does not contribute in the triplet configuration because it requires the conservation of spin at each vertex.

We see from Eqs. (25) and (26) that in the screened Hartree-Fock approximation for the irreducible electron-hole pair, the main role for the CDW as well as the SDW instabilities is played by the screened electron-hole attraction V^s, which tends to promote the creation of a large number of excitons in the ground state, leading to the usually called "excitonic" instability.[21,12]

A point that we have not considered in our formulation so far is the contribution of the electron-phonon coupling. This coupling can change the character of the instabilities. In general, the SDW instability is expected to appear before the CDW instability develops, when the electron-phonon coupling is absent, because the singlet configuration contains the repulsive term V^c.[22] This aspect will be considered in a planned subsequent publication, where we first obtain the phonons of the ideal surface system based on the same microscopic formulation of the response function.

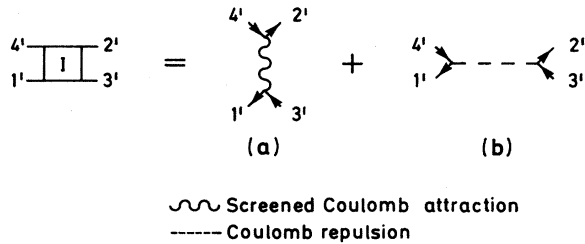Conditions similar to (25) and (26) were already ob-

Screened Coulomb attraction

------ **Coulomb repulsion**

FIG. 2. Irreducible electron-hole interaction. (a) Electron-hole screened attraction, and (b) bare Coulomb repulsion.
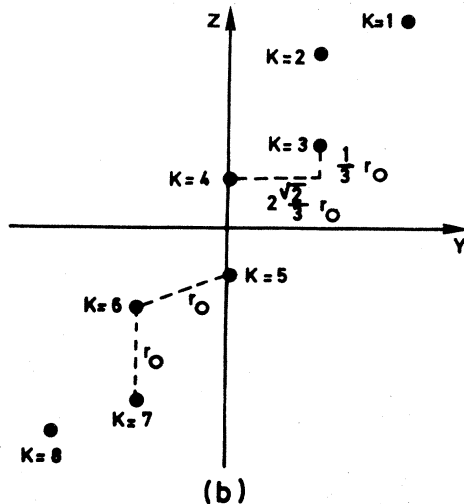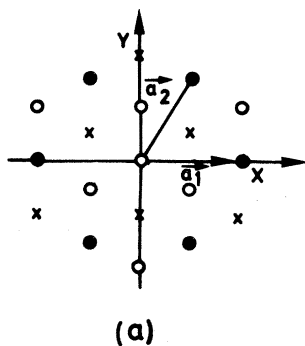

(a)

(b)

FIG. 3. Si(111) ideal slab. (a) Horizontal projection: O denotes atoms in the first, sixth, and seventh layers, X denotes atoms in the second, third, and eight layers, and ● denotes atoms in the fourth and fifth layers. a_1 and a_2 are primitive translation vectors. (b) Side view of the basis for eight layers. r_0 is the next-nearest-neighbor distance in Si.
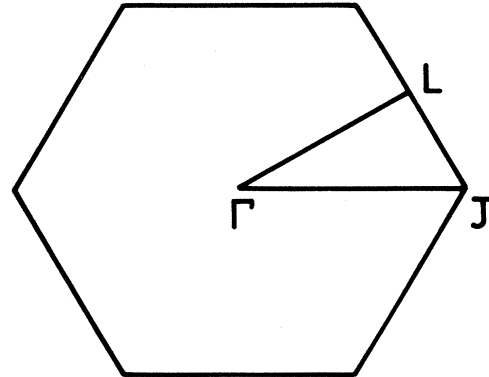

FIG. 4. Hexagonal Brillouin zone. The irreducible part is delimited by the line $\Gamma - L - J - \Gamma$.

tained by a number of authors[22-24] in the case of bulk solids. However, here we would like to emphasize two ingredients of our surface formulation. Firstly, by considering a realistic band structure, we are able to deal with the actual geometric properties of the Fermi surface. This point is of particular importance for surface systems, where the 2D Fermi surface can often present '"nesting" features, due to lowering of dimensionality. Secondly, our treatment accounts for the contributions of the direct and exchange Coulomb interactions self-consistently through the solution of the Bethe-Salpeter equation. In this way we can quantitatively follow the modification of these contributions going from the bulk to the surface.

The application to ideal Si(111), which is discussed in the next two sections, can be taken as direct evidence for the importance of these two ingredients.

III. IDEAL Si(111) SLAB: CALCULATION SCHEME

In this section we present details of the numerical study for an ideal Si(111) slab with eight layers. The unit cell of the ideal Si(111) slab was chosen as in Ref. 25, where the symmetry properties of such a system are discussed. A top view of the unit cell is shown in Fig. 3(a), with the 2D primitive translation vectors $\vec{a}_1$ and $\vec{a}_2$. Figure 3(b) is a side view of the unit cell and the coordinate system which has the following properties: (i) the origin coincides with the inversion center of the slab; (ii) the z direction is perpendicular to the slab; (iii) all the atoms in the unit cell are on the y-z plane, which is a reflection plane; and (iv) the 3D basis vectors can be obtained from Ref. 25. The Brillouin zone and its irreducible part are shown in Fig. 4.

A. Band structure and wave functions

The surface band structure (Fig. 5) was obtained in a tight-binding scheme where we considered up to fourth-nearest neighbors.[26] The parameters (Table I) were determined with a least-squares fit to the self-consistent pseudopotential results of Refs. 27 and 28 and to a self-consistent band structure for perfect silicon in a superlattice configuration with generalized Wannier functions.[29] The dangling-bond band, which appears in the band gap of Fig. 5, was fitted to the results of Appelbaum and Ha-

TABLE I. Least-squares-fitted parameters for an eight-layer Si(111) slab. $\nu, \nu' = 1$ correspond to a bond pointing in the [111] direction, and $\nu' = 2$ to a bond pointing in the [1$\bar{1}\bar{1}$] direction. The vector $\vec{R}$ is given in units of the bulk lattice constant.

Parameter	ν	ν'	$\vec{R}$	Valence band	Conduction band	DB—valence-band interactions	DB—conduction-band interactions	DB-DB interactions
ϵ_0	1	1	(0,0,0)	−5.39	5.43	0.00	0.00	0.4
ϵ_1	1	2	(0,0,0)	−1.13	−0.62	−1.28	−0.14	
ϵ_2	1	2	(1,1,0)	0.68	−0.27	0.47	−0.31	
ϵ_3	1	1	(1,1,0)	−0.20	0.16	−0.06	0.27	
ϵ_4	1	1	(1,$\bar{1}$,0)	−0.27	0.28	0.00	0.00	
ϵ_5	1	2	(1,$\bar{1}$,0)	0.01	0.25	0.02	−0.02	
ϵ_6	1	2	(0,1,$\bar{1}$)	0.00	−0.04	0.09	0.07	
ϵ_7	1	2	(0,$\bar{1}$,$\bar{1}$)	0.01	−0.11	−0.11	−0.15	
ϵ_8	1	1	(2,0,0)	−0.06	0.13	−0.07	0.08	0.058
ϵ_9	1	2	(2,0,0)	−0.22	0.15	−0.15	−0.10	

man[30] in order to describe the surface states more precisely. We obtained good overall agreement for the DB band[30] and the band complex of the valence bands.[28,29] For the conduction bands good agreement is achieved for the lowest band,[28] but unfortunately there is not detailed calculation available for the higher states. The wave functions are expanded in terms of a dangling bond, four bonding, and four antibonding orbitals, which are obtained as combinations of sp^3 hybrids. Such a description of the wave functions has been shown to be appropriate for our investigations of the dielectric properties of silicon bulk taking into account the many-body effects[4,6] and for studies of the electronic states of the surface.[31] Here, we only roughly outline the orbital determination, details of which can be found in Ref. 4. Ideally, we should have determined the single-particle spectrum and therefore orbital Gaussian coefficients in accordance with the two-particle spectrum determined from the Bethe-Salpeter equation.[5] This requires the fulfillment of a Ward identi-

ty, relating the self-energy to the irreducible vertex in Eq. (12). Clearly, this is still an impossible task and we had to resort to a pragmatic choice of single-particle energies and wave functions. Initially, the orbitals were chosen, as in our bulk studies,[4,6] by fulfilling the requirement of current conservation. In order to avoid orthogonality corrections,[5] which would render our surface calculation a formidable, extremely time-consuming task, we furthermore found it necessary to contract the bulk orbitals to more localized ones. This choice was guided by an empirical adjustment to the valence charge density of various Si bulk calculations,[32] with a typical density profile given in Fig. 6. The value of the coefficients for the Gaussian representation are given in Table II.

B. Matrices $\underline{N}$, $\underline{V}^c$, and $\underline{V}^s$

The band structure described in Sec. III A is used to calculate the noninteracting propagator $N_{ss'}$ [Eq. (16)]. We distinguish three different contributions calculated using different integration techniques in order to obtain a comparable accuracy for all of them. The most accurate method, a 2D adapted tetrahedron method,[33] was used to
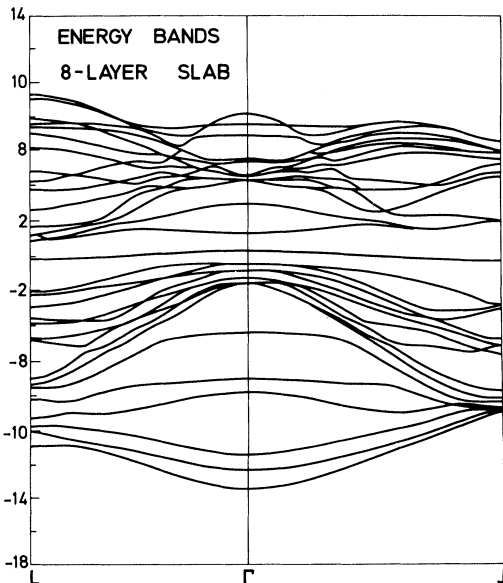
FIG. 5. Band structure in the tight-binding approximation for an eight-layer slab. The DB band appears in the gap.
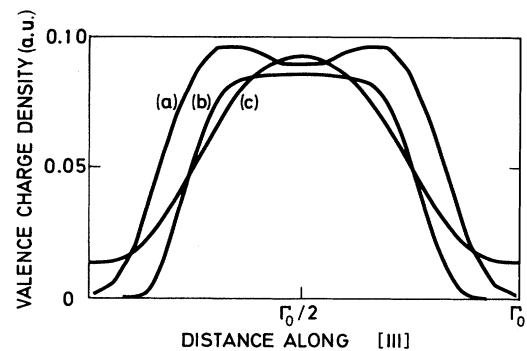
FIG. 6. Valence-band charge density along a bond. (a) This work, (b) "hard-core" pseudopotential, and (c) "soft-core" pseudopotential. (b) and (c) were obtained from Ref. 32.

TABLE II. Coefficients of Gaussian orbitals.

Wave function	Amplitude	Exponential factor
s	$a_1 = 1.3406$	$\alpha_1 = 0.3172$
	$a_2 = -1.3406$	$\alpha_2 = 1.3172$
p	$b_1 = 0.2471$	$\beta_1 = 0.502$
	$b_2 = 0.2429$	$\beta_2 = 0.155$

calculate the intraband contribution from the metallic DB band, where the denominator in Eq. (16) becomes very small for transitions in the vicinity of the Fermi surface. For interband transitions between the DB band and the valence or conduction bands we used 18 special points in the irreducible part of the 2D hexagonal Brillouin zone (BZ).[34] The contributions from interband transitions between valence and conduction bands were obtained by the "mean-value point" technique for two dimensions.[34] The overall change in the matrix elements for the last type of transition, going from 1 (mean-value point) to 18 special points, is around 1%; much more pronounced is the variation in the matrix elements corresponding to transitions between the DB band and the valence or conduction bands, with changes going up to factors of 2.

For the matrices $V^c_{ss'}(\vec{q})$ and $V^s_{ss'}(\vec{q})$ only contributions up to next-nearest neighbors in the index s were considered, the other contributions being, as in bulk,[4] at least 1 order of magnitude smaller. With this approximation the dimension of the matrices N, V^c, and V^s is 113×113. Another approximation reducing the computational effort significantly consisted of retaining only the terms corresponding to $\mu = \nu = \mu' = \nu'$ or $\mu = \mu', \nu = \nu'$ ($\mu \neq \nu$) in the indices s. With our set of Gaussian orbitals these terms are a factor of about 10 larger than the others, a result which is consistent with the bulk studies of Ref. 4.

The matrix $\underline{V}^c$ was calculated according to Eq. (19) which, in combination with the Gaussian basis, ensures a fast convergence ("Ewald summation"), as opposed to the form in Eq. (18), where the long-range character of the Coulomb interaction appears explicitly.

As can be seen from Eq. (22), the screened electron-hole interaction $\underline{V}^s$ has the same form as in the bulk, the explicit expressions being already presented in Ref. 4. We approximated the screening function in $\underline{V}^s$, $\epsilon(r,r')$, by the bulk spherical dielectric function.[4,5] For the matrix elements in V^s containing contributions from the DB surface state we have chosen the screening such that in the long-range limit ($|\vec{r} - \vec{r}'| \gg a$) a macroscopic dielectric constant with $\epsilon_0^{surf} = \epsilon_0^{bulk}/2$ results. This choice, which is not rigorous, was made in order to preserve the short-range properties of $\epsilon(r,r')$ similar to those in bulk, guided by the fact that the short-range electronic configuration of the Si(111) surface remains very similar to that in bulk.[27,35] In principle, we should have used the full dielectric function also in the electron-hole vertex (Fig. 2) $\epsilon_\omega(\vec{q}+\vec{G}, \vec{q}+\vec{G}';z,z')$. The above static and isotropic approximation proved to be a reasonable one in bulk covalent semiconductors.[4,5]

IV. ELECTRONIC INSTABILITIES IN AN IDEAL Si(111) SLAB

The formalism discussed in Sec. II is applied in a first step to a strictly 2D system which consists of a 2D array of DB orbitals with the same configuration as in the topmost layer of the ideal Si(111) slab. The aim of this effort is to isolate the contributions of the metallic surface state from the substrate and to observe in a simplified model the competition of band-structure (single-particle) and many-body (two-particle) effects.

The possibility that 2D Fermi-surface nesting is responsible for a CDW-type instability has been put foward by Tosatti and Anderson.[36,37] The Fermi surface constructed from the band structure of Sec. III is shown in Fig. 7, where no appreciably flat segments are observed. More insight is obtained by calculating the noninteracting susceptibility $N(\vec{q}, \omega = 0)$ [see Eq. (16)].

In this 2D model, with only one orbital, we restrict the calculation to terms with $R_l = R_{l'}$ in the index s (defined in Sec. II) due to the high localization of the DB orbitals.[35] Then, $N(\vec{q})$ reduces to a scalar quantity. The band structure of the system is obtained from the more complicated one of Sec. III (Fig. 5) by isolating the surface state. The integration in the BZ was carried out as described in Sec. III for wave vectors $\vec{q}$ along the symmetry directions of the irreducible part of the BZ.

The quantity $N^{-1}(q)$ is displayed in Fig. 8 (dotted line). We observe that the uncorrelated electron-hole transitions give rise to minima near wave vectors corresponding to the (7×7) reconstruction. However, the effects of nesting of the Fermi surface[36,37] are not sufficient to fulfill the condition for an electronic instability, Eq. (25), without incorporating the many-particle interaction V_{xc}. Furthermore, no structure corresponding to the (2×1) reconstruction is observable.

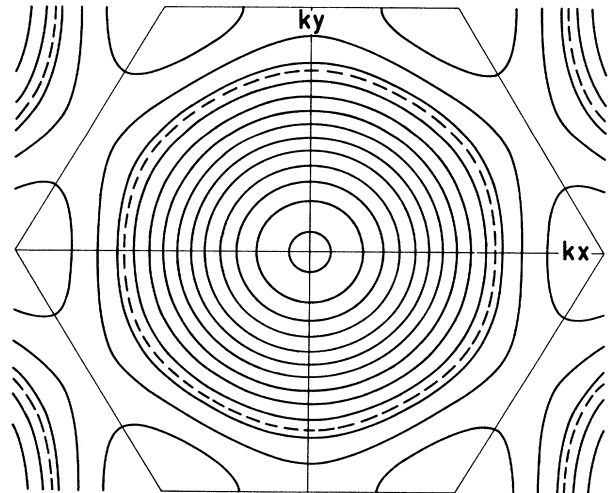To study the many-body effects, we consider the function

FIG. 7. Surfaces of constant energy for the 2D array of dangling bonds. The dashed line is the Fermi surface.
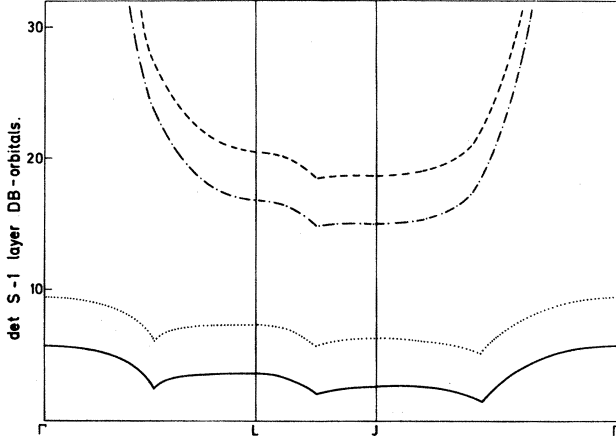
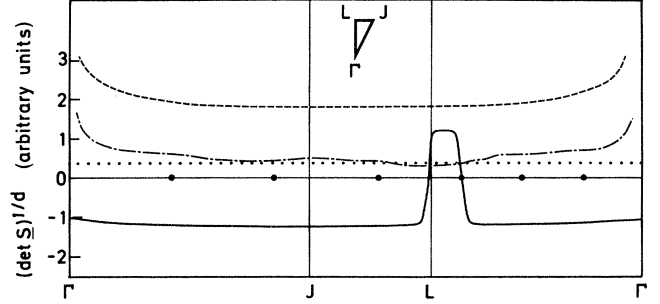FIG. 8. Inverse 2D susceptibility. For an explanation, see Sec. IV.

FIG. 9. SDW instabilities on the ideal Si(111) slab. For an explanation, see Sec. IV. The inset shows the irreducible part of the 2D Brillouin zone. The dots on the abscissa correspond to wave vectors for the possible (7×7) superstructures along the $\Gamma - J - L - \Gamma$ line.

$$S(q) = N^{-1}(q) + V^{xc}(q) . \tag{27}$$

In a first step, we take into account only the local-field effects in the RPA, i.e., $V^{xc}(q) = -V^c$. A large correction is obtained in Fig. 8 (dashed line), due to the localized nature of the DB orbitals. Most of the features present before are eliminated and the system is even further away from an electronic instability. Beyond the RPA the situation is not decisively changed. Although the electron-hole attraction pushes the curve to lower values (dashed-dotted line in Fig. 8), the system remains far from an instability.[38] Only when we consider the triplet configuration (solid line) for the electron-hole pair, where the repulsive part V^c is absent, does the system show a tendency towards an instability near wave vectors corresponding to the 7×7 superstructures. There, we are not able to reach an electronic instability (CDW or SDW) in a strictly 2D model, neither from just nesting nor by additionally including the two-particle many-body effects.

The situation is completely different in a 3D thin slab. Now $\underline{S}(q)$ is a matrix with dimensions $d \times d$ ($d = 113$ in our case), as given by Eqs. (25) and (26). Figure 9 presents a plot of $(\det \underline{S})^{1/d}$ for the same approximations as in the 2D case. The power $1/d$ was adopted in order to facilitate plotting of the different many-body approximations, which result in order-of-magnitude changes in the determinant of S, on one and the same scale. The dotted line in Fig. 9 corresponds to the Hartree approximation ($V^{xc} = 0$), and thus contains only the effects induced by the slab band structure in Fig. 5. It can be seen that, although the DB band itself produces some features due to nesting as before, they are eliminated by the interaction with the substrate and by the substrate itself. When the RPA local-field effects (Fig. 9, dashed line) are taken into account, the (1×1) paramagnetic structure becomes even more stable. This is due to the repulsive character of the interactions. A $1/q$ divergence is obtained at the Γ point. This is a result of the metallic nature of the DB band of the ideal surface. The dashed-dotted line in Fig. 9 finally shows the decisive influence of excitonic effects: The determinant becomes smaller at the zone boundary ($J - L$

line), and even smaller than in the Hartree approximation around the L point.[39] This suggests that the system has a tendency towards a CDW instability in that region. It should be stressed that our treatment (Sec. II) does not consider the coupling of the charge-density fluctuations to the ions. This is required for local charge neutrality and can trigger the appearance of a CDW instability.[22] In fact, in a previous calculation[40] of the phonon spectrum for the same system, which incorporated the above many-body effects, an instability around the L point was obtained. This is connected with a (2×1) superstructure.

Next, we consider the spin-density fluctuations (solid line) in Fig. 9. It is evident that the inclusion of the electron-hole attraction leads to two types of instabilities. The determinant goes through zero at wave vectors near those corresponding to the (2×1) and (7×7) superstructures, where the first one agrees with pseudopotential local-spin-density results.[16] To our knowledge, the (7×7) SDW instability is reported here for the first time. It would be interesting to independently study such a possi-
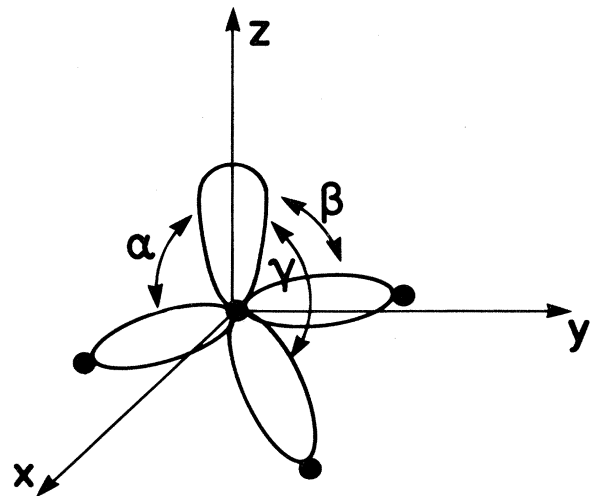

FIG. 10. Schematic representation of transitions between DB orbitals and backbond orbitals.

TABLE III. Amplitude "per site" squared for the magnetic instability. For an identification of the quantities α, β, and γ, see Fig. 10.

Transition	DB bonding	DB antibonding
α	1.47×10^{-4}	1.31×10^{-3}
β	7.60×10^{-2}	4.233×10^{-1}
γ	7.60×10^{-2}	4.233×10^{-1}

bility with the local-density ground-state methods used in Ref. 16. However, again it should be noted that we can only aim at predicting what drives the instability initially.

As a last point, we discuss the localization of the magnetic instability. This we obtain from the amplitude of elementary excitations as defined in Sec. II. The amplitude becomes especially important for surface systems and allows us to separate extended bulklike excitations from those localized at the surface. In order to obtain the amplitude "per site," F_s [Eq. (14)], we first diagonalize the matrix $\underline{S}(\vec{q})$ for the wave vector where the determinant goes to zero, and then look for the eigenvector corresponding to the zero eigenvalue. One eigenvalue is obtained around the value $\sim 0.5 \times 10^{-7}$, which is well separated from the total set ranging from $\sim 0.6 \times 10^{-1}$ to ~ 6 in absolute values. The corresponding eigenvector shows components different from zero only for those transitions between bonding or antibonding states of the backbond and the DB states on the same site (see Table III and Fig. 10). A remarkable point is that the amplitude corresponding to on-site transitions of the DB states is zero. Furthermore, we can see from Table III that the sum of the squared amplitudes for transitions between backbonds and DB states gives 1 (we took orthonormalized vectors). This demonstrates that only those transitions which are localized at the surface contribute to the instability. This fact, together with our results for the 2D model, proves that 2D models do not reproduce the physical mechanisms that trigger the electronic instabilities.

V. SUMMARY

This paper is devoted to a many-body description of surface elementary excitations. An aim has been to develop and carefully test a Green's-function formalism for surface systems with strongly inhomogeneous charge-density profiles. This formalism allows for a theoretical study of various electronically related elementary excitations which arise from a linear-response process. These excitations include plasmons, excitons, magnons, and, when complemented by the electron-lattice interaction, phonons and polarons as well. The latter interaction will be incorporated in a subsequent publication. Only then can we conclusively establish the existence or nonexistence of a CDW instability, which is favored by electron-lattice coupling.

We take into account two types of many-particle interactions: Firstly, the RPA local-field effect, which results from the electronic density fluctuations on a microscopic scale, and secondly, the screened electron-hole attraction. From the equation of motion for a surface elementary excitation its energy spectrum and amplitude are obtained. This last quantity is of particular relevance for a surface system. It makes possible the distinction of collective modes localized at the surface from the extended bulklike ones.

In a first step, we apply this formalism to the study of electronic instabilities on covalent semiconductor systems, specifically on the ideal Si(111) surface. For this surface both local-field and excitonic effects give corrections to the polarizability determinant which are of comparable magnitude to the noninteracting electron-hole contributions and are even more pronounced than in bulk.[3-6] In fact, detailed numerical studies demonstrate that they are *the* driving force responsible for the electronic instabilities obtained at the ideal Si(111) surface. Another aspect which emerges from our study is the importance of the 3D character of the system: The surface instabilities have their origin in the interactions between the first and the second layers and they cannot be reproduced in a strictly 2D model. This fact is shown explicitly by the amplitude "per site" obtained for the collective mode which corresponds to the magnetic instability. This result agrees qualitatively with Ref. 16, where a nonzero valence spin density is found up to the third layer. For the CDW-type excitations, no instability was obtained. However, CDW's could be favored if electron-phonon coupling is taken into account. This point will be taken up in a following paper.

Finally, some comments should be made concerning recent work[16-19] on reconstruction of the Si(111)2×1 surface. Owing to the fact that our formalism is devised as linear response, we can only test the stability of a given (for example, ideal) surface geometry against small disturbances against charge or spin reorientation. Nevertheless, the magnetic instability obtained for the ideal Si(111) surface is in accordance with local-spin-density calculations[19] which seem to show that a magnetic (2×1) superstructure gives a local minimum in the total energy with respect to small distortions around the ideal configuration. Future work will be directed to calculating the spectrum of elementary excitations starting from one of the different proposed models and then testing the proposal against optical[41] and photoemission experiments,[14,15] as was already successfully done in bulk.[3-6]

[1]D. Pines and P. Nozières, *Theory of Quantum Liquids* (Benjamin, New York, 1966), and references therein.

[2]P. Nozières, *Interacting Fermi Systems* (Benjamin, New York, 1964).

[3]For a review related with the effects in optical-spectrum, phonon excitations as well as broken-symmetry behavior (superconductivity and charge-density wave), see W. Hanke, Adv. Phys. **27**, 287 (1978).

[4]W. Hanke and L. J. Sham, Phys. Rev. B **21**, 4656 (1980).

[5]G. Strinati, H. J. Mattausch, and W. Hanke, Phys. Rev. Lett. **45**, 290 (1980); Phys. Rev. B **25**, 2867 (1982).

[6]H. J. Mattausch, W. Hanke, and G. Strinati, Phys. Rev. B **26**, 2302 (1982).

[7]M. Jonson and G. Srinivasan, Phys. Scr. **10**, 262 (1974).

[8]A. L. Fetter and J. D. Walecka, *Quantum Theory of Many-Particle Systems* (McGraw-Hill, New York, 1971).

[9]For surface response functions, see, for example, P. Hertel, Surf. Sci. **69**, 237 (1977); M. Nakayama, J. Phys. Soc. Jpn. **39**, 265 (1975). In the case of metals, the semi-infinite jellium model was extensively investigated. See, for example, P. J. Feibelman, Phys. Rev. B **22**, 3654 (1980), and references therein. For the case of insulators, see V. V. Hyzhnyakov, A. A. Maradudin, and D. L. Mills, Phys. Rev. B **11**, 3149 (1975); A. D'Andrea and R. del Sole, Solid State Commun. **30**, 145 (1974).

[10]P. J. Feibelman, Phys. Rev. B **9**, 5077 (1974).

[11]L. J. Sham and T. M. Rice, Phys. Rev. **144**, 708 (1966).

[12]W. Kohn, in *Many-Body Physics,* edited by C. Dewitt and R. Balian (Gordon and Beach, New York, 1968), p. 353.

[13]For recent reviews, see W. Mönch, Surf. Sci. **86**, 672 (1979); D. J. Chadi, *ibid.* **99**, 1 (1980).

[14]F. J. Himpsel, P. Heimann, and D. E. Eastman, Phys. Rev. B **24**, 2003 (1981); F. J. Himpsel and D. E. Eastman, Phys. Rev. Lett. **49**, 849 (1982).

[15]R. I. G. Uhrberg, G. V. Hansson, J. M. Nicholls, and S. A. Flodström, Phys. Rev. Lett. **48**, 1032 (1982); **47**, 850 (1982).

[16]J. E. Northrup, J. Ihm, and M. L. Cohen, Phys. Rev. Lett. **47**, 1910 (1981).

[17]K. C. Pandey, Phys. Rev. Lett. **47**, 1913 (1981); **49**, 223 (1982).

[18]New results can also be found in Proceedings of the 9th Annual Conference on the Physics and Chemistry of Semiconductor Interfaces [J. Vac. Sci. Technol. **21**, (1982)].

[19]J. E. Northrup and M. L. Cohen, in *Proceedings of the 16th International Conference on the Physics of Semiconductors, Montpellier, France, 1982,* edited by M. Averous (North-Holland, Amsterdam, 1983).

[20]A. A. Abrikosov, L. P. Gor'kov, and I. E. Dzyaloshinski, *Methods of Quantum Field Theory in Statistical Physics* (Prentice-Hall, Englewood Cliffs, N.J., 1964).

[21]D. Jérome, T. M. Rice, and W. Kohn, Phys. Rev. **158**, 462 (1967).

[22]B. I. Halperin and T. M. Rice, in Solid State Physics, edited by F. Seitz, D. Turnbull, and H. Ehrenreich (Academic, New York, 1968), Vol. 21, p. 115.

[23]P. A. Fedders and P. C. Martin, Phys. Rev. **143**, 245 (1966).

[24]S. K. Chan and V. Heine, J. Phys. F **3**, 795 (1973).

[25]S. E. Trullinger and A. A. Maradudin, Phys. Rev. B **10**, 1350 (1974).

[26]The band-structure program was provided by M. J. Kelly. It is based on a scheme developed by L. M. Falicov and F. Yudurain, J. Phys. C **8**, 147 (1975); **8**, 1563 (1975).

[27]M. Schlüter, J. R. Chelikowsky, J. G. Louie, and M. L. Cohen, Phys. Rev. B **12**, 4200 (1975).

[28]M. Schlüter and M. L. Cohen, Phys. Rev. B **17**, 716 (1978).

[29]J. Sánchez-Dehesa, J. A. Vergés, and C. Tejedor, Phys. Rev. B **24**, 1006 (1981).

[30]J. A. Appelbaum and D. R. Hamann, Phys. Rev. Lett. **31**, 106 (1973).

[31]R. del Sole and W. Hanke, Solid State Commun. **31**, 949 (1979).

[32]D. R. Hamann, Phys. Rev. Lett. **42**, 662 (1979).

[33]G. Lehman and M. Taut, Phys. Status Solidi B **54**, 469 (1972); O. Jepsen and O. K. Andersen, Solid State Commun. **9**, 1763 (1971); J. Rath and A. J. Freeman, Phys. Rev. B **11**, 2109 (1975).

[34]S. L. Cunningham, Phys. Rev. B **10**, 4988 (1974).

[35]J. A. Appelbaum and D. R. Hamann, Rev. Mod. Phys. **48**, 479 (1976).

[36]E. Tosatti and P. W. Anderson, Solid State Commun. **14**, 713 (1974).

[37]E. Tosatti, *Festkörperprobleme XV,* Vol. 113 of *Advances in Solid State Physics,* edited by J. Treusch (Pergamon, Vieweg, 1975).

[38]In a previous communication (Ref. 40) a numerical error was present in the calculation of V^{xc}, leading to greater values of this quantity for the DB-DB interactions.

[39]Note that the reduction of $(\det \underline{S})^{1/d}$ of ~ 0.1 signifies a reduction of > 6 orders of magnitude in $\det \underline{S}$.

[40]A. Muramatsu and W. Hanke, Solid State Commun. **42**, 537 (1982).

[41]G. Chiarotti, in *Recent Developments in Condensed Matter Physics,* edited by J. T. Devreese (Plenum, New York, 1981), Vol. 1, p. 633, and references therein.